JOURNAL OF MATERIALS SCIENCE 20 (1985) 624–629

Initial clustering after quenching in AlZnMg alloys

A. JUHÁSZ, I. KOVÁCS, J. LENDVAI, P. TASNÁDI
Institute for General Physics, Loránd Eötvös University, Budapest, Hungary

After solution treatment and quenching a fast increase in hardness takes place in Al–Zn–Mg alloys in the first few minutes of ageing at or near room temperature. The kinetics of this process have been studied on a number of different compostition alloys by microhardness measurements between 246 and 295 K and by resistivity measurements between 263 and 323 K. On the basis of the observed microhardness and resistivity kinetics the activation energy of the process was determined. According to this the ageing process starts with the diffusion of zinc atoms to magnesium atoms and Guinier–Preston zones develop from the so formed Mg–Zn clusters. The average Mg/Zn ratio in the clusters is 1/4. In the alloys investigated the microhardness after 15 min ageing at room temperature can be composed simply of the contributions to the hardness of pure aluminium, $MgZn_4$ clusters and of magnesium atoms remaining in solid solution.

1. Introduction

The formation of Guinier–Preston (GP) zones in Al–Zn–Mg alloys has been studied by many authors [1, 2]. However, the results are somewhat contradictory, especially those concerning the initial period of the process. To study the early-stage processes in the decomposition of the solid solution state at lower temperatures indirect methods such as electrical resistivity and microhardness measurements are mainly used [3–9]. The hardening of Al–Zn–Mg alloys as a function of ageing time at room temperature was observed to start with an incubation period then it increases linearly with the logarithm of time, thereafter a plateau appears [5, 10]. After this another strong increase in hardness occurs [5, 11].

Electrical resistivity of Al–Zn–Mg alloys was found to increase continuously during ageing at or near room temperature after quenching and in contrast to binary Al–Zn alloys a resistivity maximum could not be detected except in alloys with very low Mg/Zn ratios [4, 12, 13].

In a recent paper we have reported that in Al–Zn–Mg alloys at the very beginning (during the first few minutes) of ageing at room temperature, clusters with an average composition of $MgZn_4$ are formed [14]. In the present paper we describe results of further investigations concerning the kinetics of this initial clustering process. The investigations were extended to binary Al–Zn and Al–Mg alloys as well as to a series of Al–Zn–Mg alloys with concentration ratio, Zn/Mg = 2.

2. Experimental procedure

The specimens used in the investigations were prepared of 99.99 or 99.999% purity aluminium and of 99.99% purity alloying material. The compositions of the alloys are given in Table I. Thin sheets of thickness 1.0 and 0.2 mm for the microhardness and electrical resistivity measurements, respectively, were solution heat-treated at 480° C for 30 min and quenched in room temperature water.

The microhardness (*HV*) measurements were made using Durimet-type Leitz microhardness testing equipment with a 1 N load. The measurements were started 2 min after quenching. Measurements were made *in situ* at the ageing temperature, which was stabilized to ± 1.0° C.

Electrical resistivity measurements were performed at 78 K by the standard potentiometric method. The first measurement was made 2 min after quenching. The ageing heat-treatment of the specimens was carried out in a water or alcohol

0022–2461/85 $03.00 + .12

TABLE I Composition of the alloys investigated. Alloys of number 1–9 and 10–16 were made from 5N and 4N Al respectively

Sample	Mg (at %)	Zn (at %)
1	0.61	1.01
2	1.21	1.48
3	1.67	1.86
4	3.33	2.48
5	1.50	2.00
6	2.50	4.00
7	4.00	4.00
8	2.50	6.00
9	5.00	2.50
10	0.048	1.52
11	1.42	2.62
12	1.65	3.14
13	2.14	4.09
14	2.33	4.49
15	2.41	4.54
16	2.79	5.58

bath thermostated with an accuracy of temperature ± 0.1° C.

3. Experimental results

The changes in the diameter of the microhardness indentations in the course of room temperature ageing are shown in Fig. 1 for alloys 4, 5, 9, and 12. The decrease of the diameter indicates a fast increase in the microhardness of the samples. The rate of this initial hardening decreases continuously and a plateau is reached after about 30–40 min ageing at room temperature. During this period of time the microhardness of the samples increases between about 0–800 MPa in dependence on the alloy composition. The kinetics of the hardening process depends sensitively on the ageing temperature (Fig. 2).

The electrical resistivity of the alloys increases strongly after quenching (Fig. 3). The observed resistivity curves are typical for aluminium alloys in the case of GP zone formation [3, 4, 8, 9].

4. Discussion

The variation of the indentation diameter in the initial hardening process could be fitted to the simple expression

$$d - d_{\mathrm{pl}} = A \exp - Bt \qquad (1)$$

where d_{pl} is the diameter corresponding to the plateau in the curves, A and B are constants determined from the least square fits of the measured d values in Equation 1. The continuous lines in Fig. 1 represent the result of the

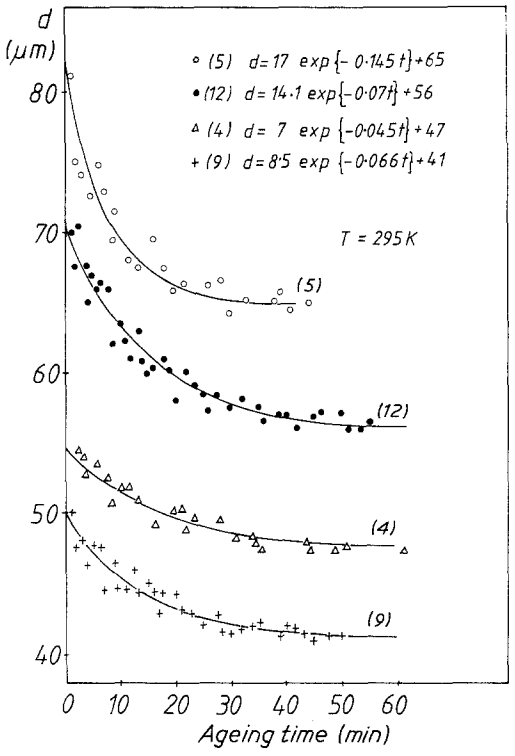

Figure 1 Variations of the diameter of microhardness indentations during room temperature ageing of alloys 4, 5, 9 and 12. The continuous lines represent the least square fit to Equation 1.

fitting. The temperature dependence of parameter B in Equation 1 can be described by the Arrhenius' Equation

$$B = B_0 \exp - Q/kT \qquad (2)$$

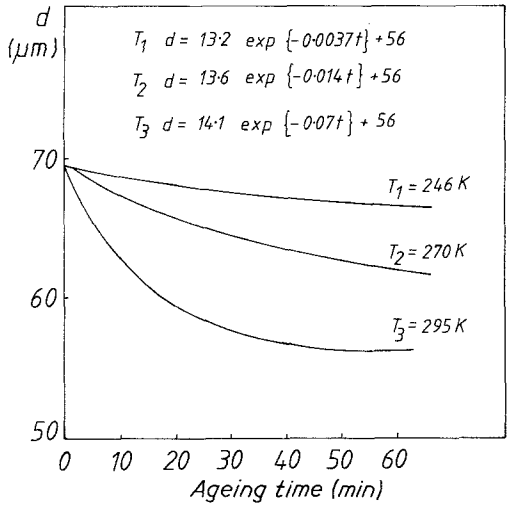

Figure 2 Isothermal variation of the indentation diameter at 246, 270 and 295 K for alloy 12.

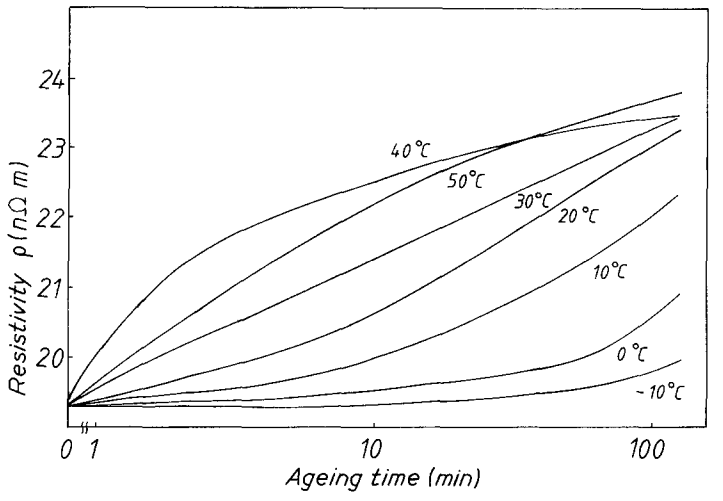

Figure 3 Changes in the electrical resistivity of alloy 12 during isothermal ageing treatments between 263 and 323 K.

From the slope of the Arrhenius plots (Fig. 4) an activation energy of 0.41 eV was obtained in case of alloys 5, 8, 9 and 12, which is close to the activation energy of Zn-migration in aluminium alloys [4, 15, 16]. On the other hand from the isothermal resistivity curves an activation energy of 0.68 eV was obtained in the temperature range -10 to $+40°$ C by the usual cross-cut method (Fig. 5). This value is close to the migration energy of magnesium [3, 4, 9].

The activation energy obtained on the basis of the microhardness measurements indicates that the strong increase in hardness during the initial clustering process at or below room temperature is connected to the migration of zinc atoms. It is probable that zinc atoms diffuse to the magnesium atoms and so the lattice strains caused by the large size of the magnesium atoms are reduced [17]. It seems that the formation of these Mg–Zn clusters does not change the resistivity of the alloy considerably and the increase in resistivity probably sets in only when two or more such clusters join to form a larger one. According to this the 0.68 eV activation energy determined from the resistivity

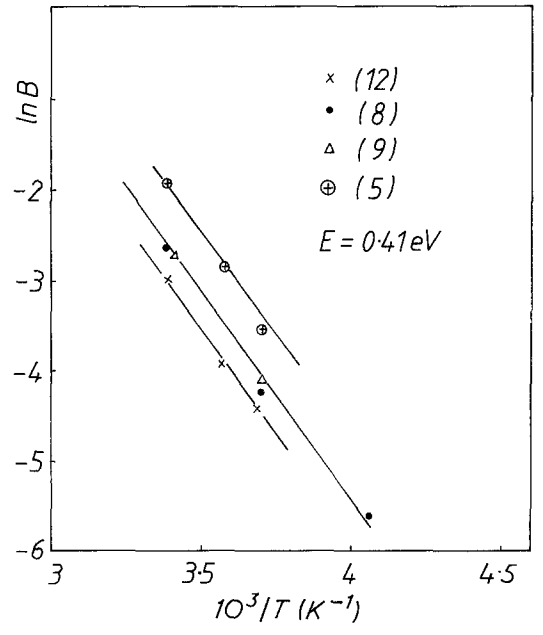

Figure 4 Determination of the activation energy from the temperature dependence of B (Equation 2).

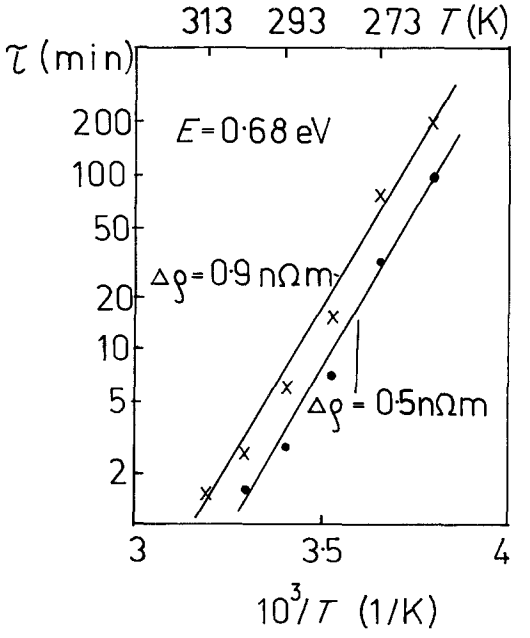

Figure 5 Arrhenius plots obtained by the cross-cut method from the resistivity curves given in Fig. 3.

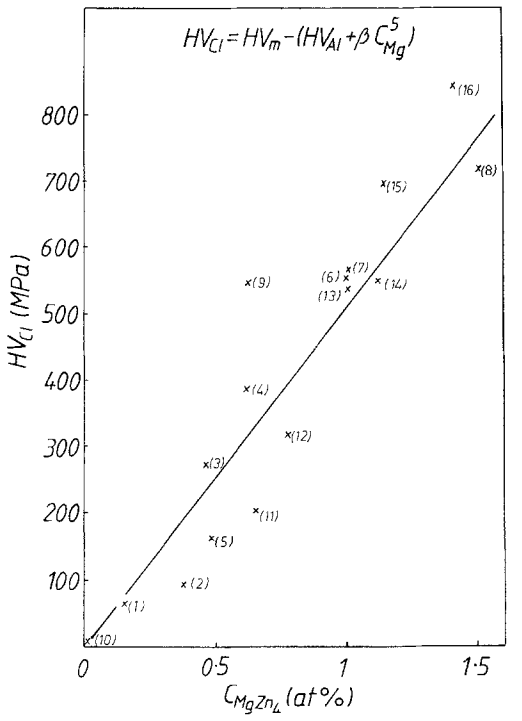

Figure 6 The hardening effect of the $MgZn_4$ clusters against the amount of clusters for the different alloys.

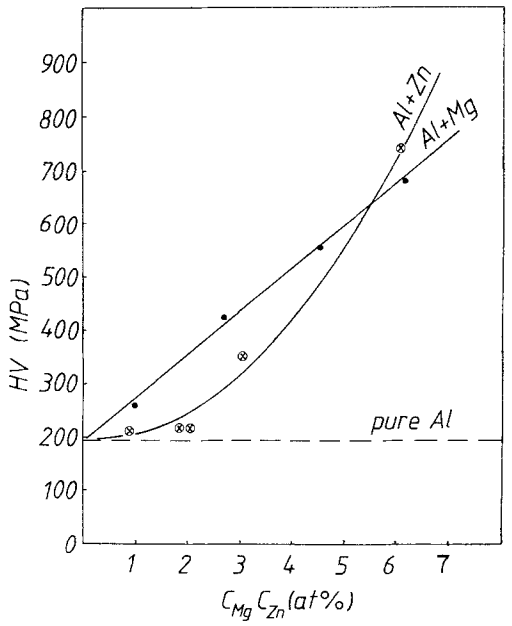

Figure 7 Microhardness of quenched binary Al–Zn and Al–Mg alloys as a function of concentration.

measurements is characteristic of the migration of the Mg–Zn clusters. The average composition of the clusters formed by the fast diffusion of zinc atoms immediately after quenching is $MgZn_4$ in accordance with our previous results [14]. This is supported by Fig. 6 where the hardening effect of the clusters is plotted against the amount of $MgZn_4$ clusters. The amount of $MgZn_4$ clusters, C_{MgZn_4}, was calculated by assuming that all the zinc atoms take part in the clustering and consequently

$$C_{MgZn_4} = \tfrac{1}{4} C_{Zn} \qquad (3)$$

if $C_{Zn}/C_{Mg} \leqslant 4$, which holds for all the alloys investigated. The hardening effect of the clusters (HV_{Cl}) was calculated by

$$HV_{Al} = HV_m - HV_{Al} - HV_{Mg}^s \qquad (4)$$

where HV_{Al} (= 200 MPa [18]) is the hardness of pure aluminium, HV_{Mg}^s is that caused by magnesium atoms remaining in solid solution, and HV_m is the hardness of the alloy measured after 15 min ageing.

To determine the hardness caused by magnesium and zinc atoms in solid solution measurements were also made on binary alloys immediately after solution treatment and quenching. Fig. 7 shows the microhardness of these alloys as a function of solute concentration. It can be seen that the hardening effect due to the solute magnesium atoms changes linearly with the solute magnesium concentration, C_{Mg}^s:

$$HV_{Mg} = \beta C_{Mg}^s \qquad (5)$$

where the proportionality factor, β, is 80 MPa/at%. The effect on hardness of solute zinc atoms increases faster than linearly with zinc concentration (Fig. 7). To determine HV_{Mg}^s in Equation 4 we used, because of Equation 3,

$$C_{Mg}^s = C_{Mg} - \tfrac{1}{4} C_{Zn} \qquad (6)$$

where C_{Mg} denotes the total alloyed magnesium concentration.

The existence of $MgZn_4$ clusters has been established already in a previous paper [14]. There we have assumed that the $MgZn_4$ clusters have no hardening effect and the entire hardness increment was attributed to the magnesium atoms remaining in solid solution. The hardening effect of solute magnesium atoms obtained in this way was much larger than that determined from previous measurements on binary Al–Mg alloys [18]. From the present analysis it is clear, however, that a definite contribution to the hardness arises also from the $MgZn_4$ clusters, and the resulting hardness is

caused by these clusters together with the remaining solute magnesium atoms.

The reason of the previous misinterpretation of the hardness increment can be seen as follows. According to Equation 4 the increment of microhardness, ΔHV, in the course of formation of $MgZn_4$ clusters can be written as

$$\Delta HV = HV_m - HV_{Al} = \alpha C_{MgZn_4} + \beta C^s_{Mg} \quad (7)$$

where the proportionality factor α is obtained from Fig. 6 to be 508 MPa/at %. Applying Equations 3 and 6 the hardness increment can be expressed as

$$\Delta HV = (C_{Mg} - C^s_{Mg})\alpha + C^s_{Mg}\beta. \quad (8)$$

If the measurements are carried out on a series of alloys in which $C_{Mg} - C^s_{Mg} \approx \gamma C^s_{Mg}$ with γ being approximately constant then a simple linear relationship between ΔHV and C^s_{Mg} can be found:

$$\Delta HV = (\gamma\alpha + \beta) C^s_{Mg} \quad (9)$$

In the alloys 1–7, investigated in our previous paper [14], γ varies between 1/3 and 1/2 and so the linear relationship between ΔHV and C^s_{Mg} could be found as a good approximation, leading therefore to the proportionality factor given in Equation 9 which is significantly higher than β. Taking the value of $\alpha = 508$ MPa/at %, $\beta = 80$ MPa/at % and as a mean value $\gamma = 0.35$, $\Delta HV = 258\, C^s_{Mg}$ is obtained which is in good agreement with the value of 264 MPa/at % obtained in the previous paper. In the series of alloys (11–16) with Zn/Mg = 2 the value of γ is 1, and the proportionality factor in Equation 9 is 588 MPa/at %. The ΔHV as a function of C^s_{Mg} is shown for the two series of alloys in Fig. 8.

From the value of α it is clear that the $MgZn_4$ clusters which form during the first few minutes of ageing at or near room temperature do have a significant hardening effect. A possible configuration of these $MgZn_4$ clusters is that zinc atoms are situated in each of the four equivalent (1 1 1) planes crossing a magnesium atom.

The hardness of quenched Al–Zn–Mg alloys changes quickly after quenching (Figs. 1 and 2) and so the hardness value corresponding to the solid solution state can only be determined by extrapolating the indentation diameter against time functions to $t = 0$. It is worth mentioning, however, that the microhardness values of the solid solution alloys determined in this way can be obtained by simply adding the hardness contributions of dissolved magnesium and zinc atoms which are known from the measurements made on binary Al–Mg and Al–Zn alloys (Fig. 7). This is demonstrated by the straight line in Fig. 9, where the microhardness obtained by extrapolation is plotted against the values calculated on the basis of Fig. 7. This result indicates that immediately after quenching the state of the alloys investigated

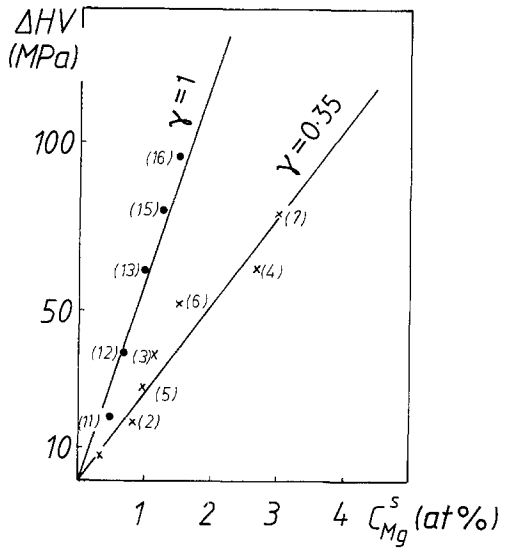

Figure 8 ΔHV as a function of solute magnesium concentration for alloys 1 to 7 ($\gamma \simeq 0.35$) and for alloys 11 to 17 ($\gamma = 1$).

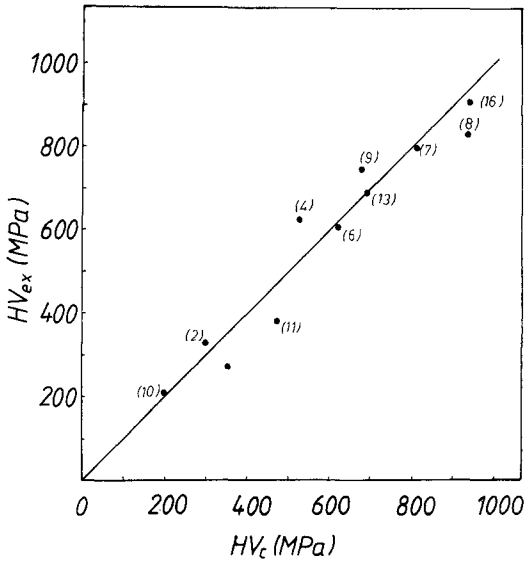

Figure 9 The microhardness corresponding to the solid solution state obtained by extrapolation (HV_{ex}) against the calculated value, HV_c obtained by adding the contributions of zinc and magnesium atoms in solid solution.

is due to the composition of the states observable in binary alloys after quenching.

5. Conclusions

In the Al–Zn–Mg alloys investigated a fast clustering process takes place during ageing at or near room temperature after solution treatment and quenching. The clustering is accompanied by a considerable hardening, the rate of which is controlled by the migration of solute zinc atoms. The analysis of the concentration dependence of the observed hardening effect indicates that the average Zn/Mg ratio in the clusters is 4:1. The contribution of these clusters to the hardness is 508 MPa/at %.

The hardness of the as quenched alloys can be composed by adding the hardness of pure aluminium and the contributions of the solute zinc and magnesium atoms which are determined experimentally from measurements on quenched binary Al–Zn and Al–Mg alloys. In the latter case the hardness increment is a linear function of concentration with a slope of 80 MPa/at %.

From the isothermal changes in the electrical resistivity a 0.68 eV activation energy was determined. This suggests that GP zone formation takes place by the migration of the Mg–Zn complexes and the rate of this process is controlled by the migration of the magnesium atoms.

References

1. L. F. MONDOLFO, *Int. Metal. Rev.* **153** (1971) 95.
2. H. LÖFFLER, I. KOVACS and J. LENDVAI, *J. Mater. Sci.* **18** (1983) 2215.
3. S. CERESARA and P. FIORINI, *Mat. Sci. Eng.* **10** (1972) 205.
4. C. PANSERI and P. FEDERIGHI, *Acta Metall.* **11** (1963) 575.
5. N. RYUM, *Ibid.* **16** (1968) 927.
6. H. G. FABIAN, P. TAPLICK and H. LÖFFLER, *Phy Status solidi (a)* **13** (1972) K169.
7. H. BOSSAC, H. G. FABIAN and H. LÖFFLER *ibid* **48** (1978) 369.
8. T. UNGÁR, J. LENDVAI, I. KOVÁCS, G. GROMA and E. KOVÁCS-CSETENYI, *J. Mater. Sci.* **14** (1978) 671.
9. E. KOVÁCS-CSETÉNYI, G. GROMA, J. LENDVAI, T. UNGÁR and I. KOVÁCS, *Aluminium* **57** (1981) 472.
10. I. J. POLMEAR, *J. Inst. Met.* **86** (1957–58) 113.
11. K. ASANO and K. HIRANO, *Trans. Jap. Inst. Met.* **9** (1968) 24.
12. H. SUZUKI, M. KANNO and S. ASAMI, *J. Jap. Inst. Light Met.* **22** (1972) 269.
13. M. OHTA and F. HASHIMOTO, *J. Phys. Soc. Jap.* **19** (1964) 130.
14. A. JUHÁSZ, P. TASNÁDI, I. KOVÁCS and T. UNGÁR, *J. Mater. Sci.* **16** (1981) 367.
15. H. G. FABIAN and H. LÖFFLER, *Phys. Status Solidi (a)* **21** (1974) 551.
16. H. G. FABIAN, R. KROGGEL, H. LÖFFLER and O. SIMMICH, *ibid.* **56** (1979) 143.
17. H. W. KING, *J. Mater. Sci.* **1** (1966) 79.
18. R. P. REED, *Cryog.* **12** (1972) 259.

Received 21 October 1983
and accepted 12 April 1984